

Synthesis and characterization of ultra-fine titania powders for wastewater treatment

S. Zahra^a, F. Deeba^b, M. Irshad^c, A. Sheikh^a, S. Zahra^{d,*}, A. M. Khan^c

^a*Mineral Processing Research Centre, Pakistan Council of Scientific and Industrial Research, Ferozpur Road, Lahore, Pakistan*

^b*Centre for Environmental Protection, Pakistan Council of Scientific and Industrial Research, Ferozpur Road, Lahore, Pakistan*

^c*Department of Chemistry, DSNT, University of Education, College Road, Township, Lahore, Pakistan*

^d*Department of Physics, DSNT, University of Education, College Road, Township, Lahore, Pakistan*

Ultra-fine titania powders were synthesized through sol-gel method. A surfactant-free non-aqueous approach was followed as a quite suitable alternative to surfactants using titanium tetrachloride and 2-ethyl hexanol as precursors. The prepared samples were calcined at different temperatures ranging from 500 °C to 800 °C. The crystal structure and thermal stability of metal oxide particles were studied using X-ray diffraction technique (XRD) and differential scanning calorimetry (DSC-TGA) respectively. The purity of powders was checked by infrared spectroscopy (IR) whereas the surface morphology was studied by field emission scanning electron microscopy (FESEM). The prepared titania samples were employed for the reduction of cyanide, BOD, COD, TDS, color and pH of industrial wastewater.

(References August 28, 2021; Accepted December 8, 2021)

Keywords: Titania, Sol-gel, Non-aqueous, X-ray diffraction, Differential scanning calorimetry

1. Introduction

Synthesis of ultrafine structures has become extremely common since last few decades. A variety of methods have therefore been developed for this purpose, including ball milling, chemical vapor deposition, physical vapor deposition, spray pyrolysis, microemulsion, electrodeposition, hydrothermal process, aerosol route and sol-gel method [1–4]. The most widespread technique among these is the sol-gel method, since it is simple and capable of producing homogeneous structures with controlled size and enhanced physico-chemical properties of nanostructures as compared to their bulk counter parts[5,6]. Generally, the precursors employed for producing nano as well as micro structures through this technique are of both organic and inorganic origin, for example, alkoxides, acetates, acetylacetonates or salts like chlorides whereas alcohols, aldehydes, ketones or oxygen-free solvents for example, amines or nitriles with short alkyl chains are used as solvents [7,8].

At present, a wide range of oxides have been developed, out of which, semiconducting materials like titania have been extensively used in photocatalysis, gas sensors, optical devices, electrodes, paints and pigments owing to their outstanding photocatalytic activity, gas-sensitivity, dielectric properties, high refractive index, chemical stability and non-toxicity. Also, titania has been employed as an antiviral and antibacterial agent for the degradation of cancer cells as well as various toxic organic compounds [9–11]. In addition to these characteristics, titania has the advantage of being economical and environmentally safe [12].

It is noteworthy that most recently, majority of the researchers have adopted aqueous sol-gel route for the synthesis of titania powders [2,13–19] despite the fact that this technique has some limitations since a strict control on various reaction parameters that strongly affect the

* Corresponding author: sarwat.zahra@ue.edu.pk

synthesis is not possible due to spontaneous hydrolysis and condensation reactions. Non-aqueous sol-gel process on the other hand, is believed to be the most promising substitute for the aqueous routes in terms of better control on particle size, shape as well as surface properties due to slower reaction rates that may result in the development of metal oxide particles with homogeneous structures and better dispersibility in organic solvents [20]. Loreyuenyoung and co-workers synthesized titania through non-aqueous route of sol-gel technique using cetyltrimethylammonium bromide surfactant as template [21]. Though surfactants are believed to control the crystallization and agglomeration but simultaneously they influence the toxicity of the product and hence, it has to be purified extensively that may significantly affect its crystal structure. Such problems can be avoided by following more simple methodologies involving use of organic solvents that are capable of being used as reactant in addition to playing a significant role as mediator for tailoring the required structure of high-purity particles [22].

In this work, a surfactant-free non-aqueous approach for the preparation of high-purity titania powders with titanium tetrachloride and 2-ethyl hexanol as precursors has been presented. The prepared samples were characterized by X-ray diffraction analysis, differential scanning calorimetry, infrared spectroscopy and field emission scanning electron microscopy. The performance of prepared titania samples was checked by applying them for the reduction of cyanide, BOD, COD, TDS, color and pH of industrial wastewater.

2. Experimental

2.1. Materials

Titanium tetrachloride used as precursor was of Merck, England whereas 2-ethyl hexanol and ethanol used were also of analytical grade.

2.2. Sample Preparation

Titania powders were synthesized via non-aqueous sol-gel route. The preparation was carried out by adding titanium tetrachloride to 2-ethyl hexanol in stoichiometric ratio to produce an alkoxide and then ethanol was added to it in 4:1 ratio to 2-ethyl hexanol. The pH was kept at 1 and the mixture was stirred constantly for one hour at 80°C. The sol thus obtained was dried at 80°C for several hours till complete drying. The dried samples were ground and then calcined for one hour at various temperatures ranging from 500 °C to 800 °C.

2.3. Characterization

Crystal structure of the prepared samples was identified by X-ray diffractometer Bruker diffractometer D8 Advance using monochromatised CuK_α radiation having wavelength of 1.5406Å. Thermal analysis was performed using differential scanning calorimeter Universal V4.5A, TA instruments USA, under nitrogen atmosphere from room temperature to 1000°C at a rate of 10°C/min. Infrared spectroscopy was carried out with Thermo Nicolet IR 200 (USA), the samples were scanned through Zinc Selenide (Zn-Se) ATR. Surface morphology studies as well as energy dispersive analysis were carried using field emission scanning electron microscope FEI Nova 450 NanoSEM.

2.4. Wastewater Treatment

2.4.1. Cyanide standard solutions

Cyanide standard solutions (10ppm and 20ppm) were prepared by making dilutions of 1000ppm Merck solution.

2.4.2. Batch Experiments

Tests were carried out to study the reduction of cyanide, BOD, COD, TDS, color and pH of industrial wastewater keeping contact time (20 hours), reaction temperature (room temperature), agitation speed (120 rpm) and agitation time (4 hours) constant. Tests were conducted in 250mL Erlenmeyer flasks containing industrial wastewater. The efficiency of synthesized TN samples was also compared by carrying out separate tests varying dosage of each sample i.e. 1g/L and 2g/L

keeping all other parameters constant. The solutions thus obtained were filtered and the residual BOD, COD, TDS, color and pH were determined in the filtrate solutions according to APHA American Public Health Association standard methods.

The reduction of cyanide was carried out in cyanide synthetic solution (10-20ppm) by applying varying dosage (1-2g/L) of TN samples. The cyanide ion was analyzed in the filtrate by cyanide testing kit Spectroquant E Merck.

3. Results and Discussion

Synthesis of high purity ultrafine titania nanoparticles was carried out via commonly used sol-gel technique. A non-aqueous route was selected for the synthesis using titanium tetrachloride and 2-ethyl hexanol as precursors since, in case of aqueous sol-gel synthesis of titania using titanium tetrachloride, it is quite difficult to control hydrolysis and condensation rate owing to the high reactivity of titanium tetrachloride towards water; its reactivity can be possibly decreased by using some functional alcohol capable of modifying the reactivity of precursor. Moreover, the process applied appears to be an appropriate alternative to surfactants due to the use of an organic solvent capable of acting as a reactant as well as a mediator for controlling particle growth thus leading to the formation of highly pure particles in a surfactant free medium [22]. Furthermore, an advantage of using 2-ethyl hexanol is that it is a high boiling liquid as compared to generally employed solvents like normal aliphatic alcohols so, at controlled temperatures it can lead to an increased viscosity of the sol resulting in slow evaporation thus producing highly porous and homogeneous structures.

It was observed that titanium tetrachloride employed as a source for titania readily reacts with 2-ethyl hexanol to form alkoxide at room temperature. The metal alkoxide precursor formed was then diluted with ethanol and the sol was prepared keeping temperature, pH and stirring time constant. In fact, the consistency of gel is strongly influenced by the operating parameters including solubility of reagents in the solvent used, order of mixing reactants, temperature and pH of the solution [7]. Particularly in sol gel method, the material formed is of amorphous nature hence, calcination at temperatures usually higher than 300°C is required to induce particle growth leading to crystallization followed by growth of crystalline particles thereby decreasing their specific surface area [18,23].

3.1. X-ray diffraction analysis

The prepared samples of TiO₂ nanopowders i.e. TN-1, TN-2, TN-3 and TN-4, calcined at 500°C, 600°C, 700°C and 800°C respectively were evaluated by X-ray diffraction technique and their diffractograms are shown in Figure 1(a, b, c & d). All the peaks were identified using DiffracPlus software for Bruker diffractometer D8 Advance that confirms the crystalline nature of all the four samples. The figure shows no other phase of titania except anatase upto 700°C calcination temperature since, the distinct peak at 2θ value 25.3° with the diffraction of [101] plane (lattice constants $a = 3.78$, $a/b = 1.0$, $c/b = 2.5$) corresponds to the tetragonal anatase phase of titania. Also, the smaller peaks at 36.9° [103], 37.8° [004], 38.6° [112], 48.1° [200], 53.9° [105], 55.1° [211], 62.1° [213], 68.8° [116], 70.3° [220] and 75.1° [215] in case of all the three TN-1, TN-2 and TN-3 samples confirm the presence of anatase [PDF 78-2486]. All these observations are in close agreement with the work of previous scientists [24].

Similar diffraction peaks for anatase phase can be observed in case of TN-4 although the peaks become narrower at higher temperatures suggesting an increased crystallite size [25] probably due to aggregation of titania crystals. The XRD pattern for TN-4 reveals the presence of rutile phase in addition to anatase which shows that with the increase in calcination temperature from 700°C to 800°C, anatase phase starts transforming into rutile phase and as the temperature reaches 800°C, a significant quantity of the titania is converted into rutile phase. This fact is evident from the presence of well-defined new peaks at 2θ values 27.4°, 36.0°, 39.1°, 41.2°, 44.0°, 54.3°, 56.6°, 62.7°, 68.9°, and 69.7° corresponding to [110], [101], [200], [111], [210], [211], [220], [002], [301] and [112] diffraction planes respectively with lattice parameters $a = 4.59$, $a/b = 1.0$, $c/b = 0.64$, which are consistent with the tetragonal symmetry of rutile phase [PDF 87-0920]. All

these 2θ values and their respective diffraction planes are quite close to that observed by Shajudheen and co-workers [26]. However, no peak for brookite phase is observed in any TN sample.

It can therefore be inferred that TN-1, TN-2 and TN-3 are purely anatase whereas TN-4 is a mixture of anatase and rutile phases of titania in almost 1:1 ratio. As observed by the previous scientists, amorphous titania transforms completely into crystalline anatase phase from 400°C to 500°C; calcination at lower temperatures on the other hand, leads to the formation of mixtures of amorphous and crystalline titania particles [16,23]. Furthermore, at 600°C conversion of anatase to rutile phase has been reported which shows that anatase phase is stable below 600°C and starts converting into small quantities of brookite and then at higher temperatures into rutile phase [13,27]. In fact, the conversion of anatase to rutile phase takes place at various temperatures ranging from 600°C to 1100°C since it depends on several factors including size of anatase crystallites and formation of brookite phase as an intermediate [21,28].

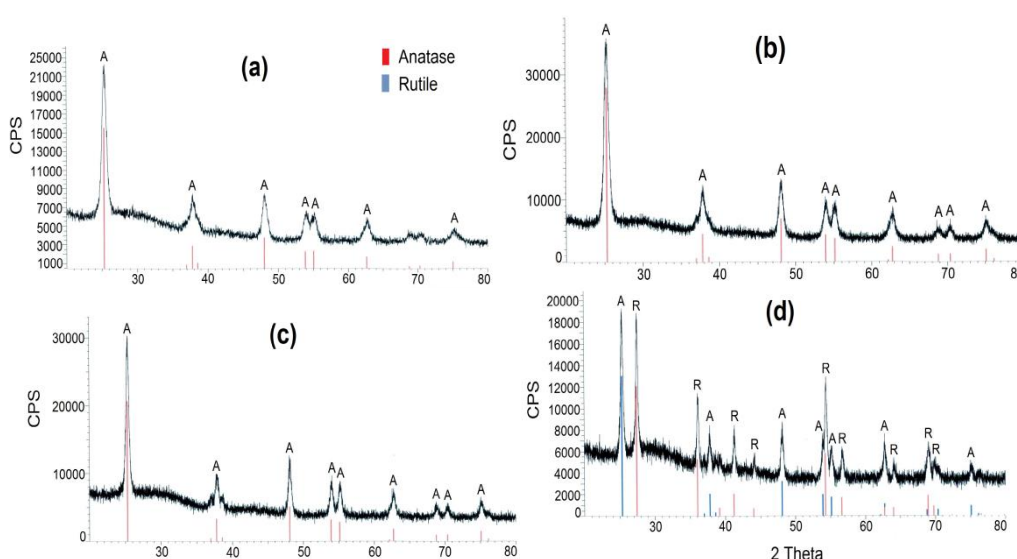


Fig. 1. X-ray diffractograms of (a) TN-1; (b) TN-2; (c) TN-3; (d) TN-4

Hence, the use of 2-ethyl hexanol as solvent inhibits the transformation of anatase to rutile phase and increases its stability upto 700°C; as concluded by Jung and co-workers [27] that heat treatment at higher temperatures without forming rutile phase leads to improved physical properties of titania due to better crystallinity. Keiteb et al. [1] on the other hand, having contrast observation concluded that photocatalytic activity improves when anatase and rutile phases co-exist owing to the utilization of electron-hole pairs among interconnecting particles of both the phases.

3.2. Thermal analysis

Thermal behavior of synthesized titania samples TN-1, TN-2, TN-3 and TN-4 was studied by DSC-TGA and curves are shown in Figures 2a, 2b, 2c and 2d respectively. The TGA curve shows a gradual but continuous weight loss of about 5.5% in case of TN-1. According to Mehranpour and co-workers [29], through sol-gel synthesis three kinds of impurities are carried with the product i.e. moisture, oxides and organic residues. Among these, moisture is adsorbed physically whereas organic residues are absorbed chemically by the material and consequently they are desorbed at different temperatures. Therefore, this total weight loss of 5.5% can be divided into three steps; the first step of about 2.5% below 200°C can be attributed to the removal of physically adsorbed moisture. The second step of minor weight loss of about 1% between 200°C and 500°C results due to the organic residues entrapped in the mesopores present between the crystallite aggregates. Ba-Abbad et al. [23] observed the complete decomposition of organic compounds from 180°C to 380°C, with about 9.0 % weight loss. Similarly, Swapna et al. [30] found 6.36% mass reduction from 300°C to 440°C, due to the loss of organic residues. Pol et al. [31] also observed the

degradation of organic groups between 250°C and 350°C. The third slight variation of 2% loss in mass from 500°C to 1000°C can be ascribed to mild phase change in anatase titania that indicates its thermal stability. However, previous scientists reported thermal stability and constant mass of anatase titania above 600-700 °C [30,32].

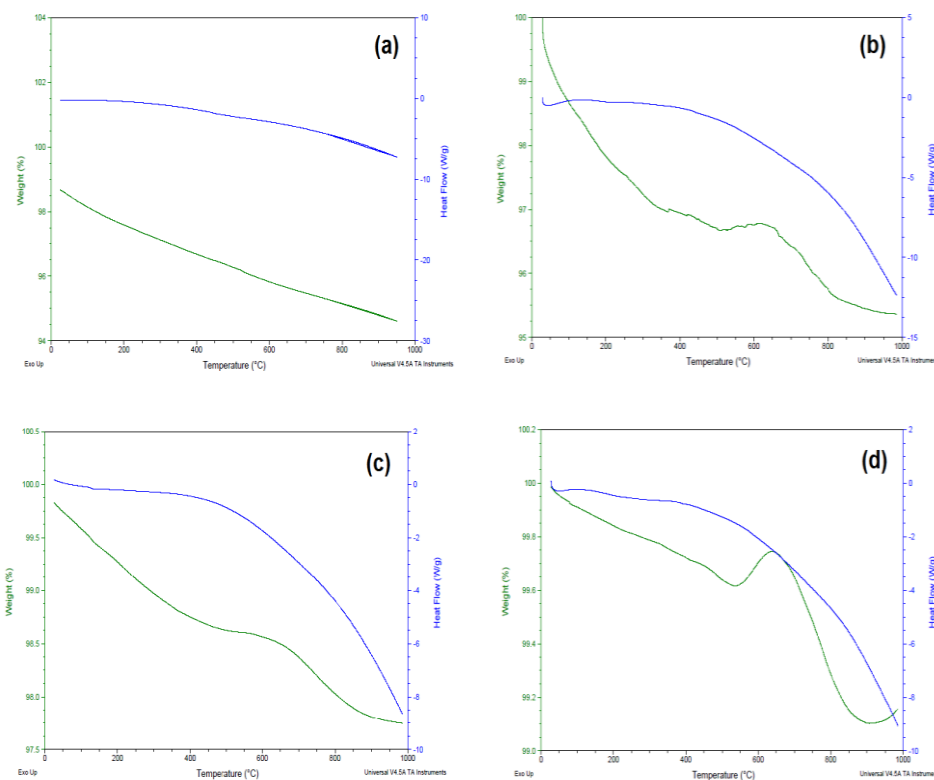


Fig. 2. DSC curves of (a) TN-1; (b) TN-2; (c) TN-3; (d) TN-4.

In case of TN-2, a total weight loss of 4.5% is observed below 500°C due to the entrapped moisture and organic residues. Unlike TN-1, an increase in weight of about 0.25% is observed from 500°C to 650°C in case of TN-2, may be due to some phase change in anatase titania that further continues from 650°C to 900°C and finally becomes stable after 900°C. For TN-3 a total weight loss of 1.5% is observed due to moisture and organic residues; the sample shows stability from 500 °C to 650 °C and another weight loss of about 0.75% between 650°C and 900°C can be ascribed to minor change in phase. The TGA curve for TN-4 shows a similar behavior as TN-2 with a minor weight loss of 0.4% below 550°C and then an increase in weight of about 0.2% from 550°C to 650°C can be observed with a successive weight loss of 0.65% between 650°C and 900°C. It is therefore evident from these results that thermal stability of the product increases with increasing calcination temperature.

Differential scanning calorimetric analysis was carried out to determine the thermal transitions in titania powders. As illustrated in Fig. 2, the DSC curve for TN-1 is almost a straight line with no exothermic peak showing that the anatase phase remains stable when calcined at 500°C. However, in case of remaining three samples i.e. TN-2, TN-3 and TN-4, the curves show thermal stability upto 650°C and then a broad exothermic peak is observed upto 1000°C that can be related to the slow transformation of anatase phase of titania to rutile among all the three samples. These results are in close agreement with the findings of previous researchers [4]. A few scientists observed the conversion of amorphous titania into anatase, though the phase change of anatase titania to rutile starts around 550°C [32]. However, in case of using low boiling solvents for titania synthesis, the transformation of amorphous titania into anatase between 400°C to 550°C has also been reported [23,31].

Hence, it can be inferred that using 2-ethyl hexanol as solvent increases the thermal stability of anatase phase till 650°C and allows slow transformation to rutile phase above this temperature. The DSC patterns also confirm the absence of brookite phase during the thermal transitions of all the four titania powders. In a previous study scientists observed that when titania starts to crystallize, anatase form appears first that further transforms into rutile phase. During this process as rutile titania starts crystallizing, the nucleation of anatase either stops or its complete conversion into rutile phase occurs. Therefore, brookite phase if forms, appears as an intermediate instead of pure brookite owing to the fact that it does not attain equilibrium under ambient conditions [33]. Hu and co-workers [34] on the other hand had a contrast observation as they obtained mixtures of anatase and brookite during the synthesis of titania powders.

3.3. Infrared spectroscopy

The IR spectra of calcined titania powders were recorded in the range of 400-4000 cm^{-1} and are presented in Fig. 3. The figure identifies that for all the four samples the region 400-1000 cm^{-1} is dominated by the intense broad absorption bands corresponding to the stretching vibrations of Ti-O and Ti-O-Ti bonds of titania network [14]. It can be noted that this broad band appears at similar positions in case of TN-1, TN-2 and TN-3 but in case of TN-4 a sharper band with some more bands specific for rutile phase can be observed that confirms the presence of multiphase structure [16].

Further, the spectra show several bands of very low intensity merged to form broad bands in the range of 1000-4000 cm^{-1} . Below 3000 cm^{-1} , these broad bands can be ascribed to the symmetric as well as asymmetric stretching vibrations of C-H bonds of entrapped organic residues. The others in the range of 3000-3600 cm^{-1} can be assigned to the combination of various vibrational modes of O-H groups originating from adsorbed water molecules as well as hydrogen bonded O-H groups. The region from 3600-3800 cm^{-1} is generally associated with stretching vibrations of O-H groups of surface adsorbed water molecules condensed in the pores of titania nanoparticles that significantly enhance their photocatalytic activity. As stated by the previous researchers, among all the surface hydroxyl groups those showing absorption band at about 3700 cm^{-1} are the most photocatalytically active [15,16]. Li et al. reported that the density of surface hydroxyl groups reduces with the reaction time during the synthesis of nanoparticles [25].

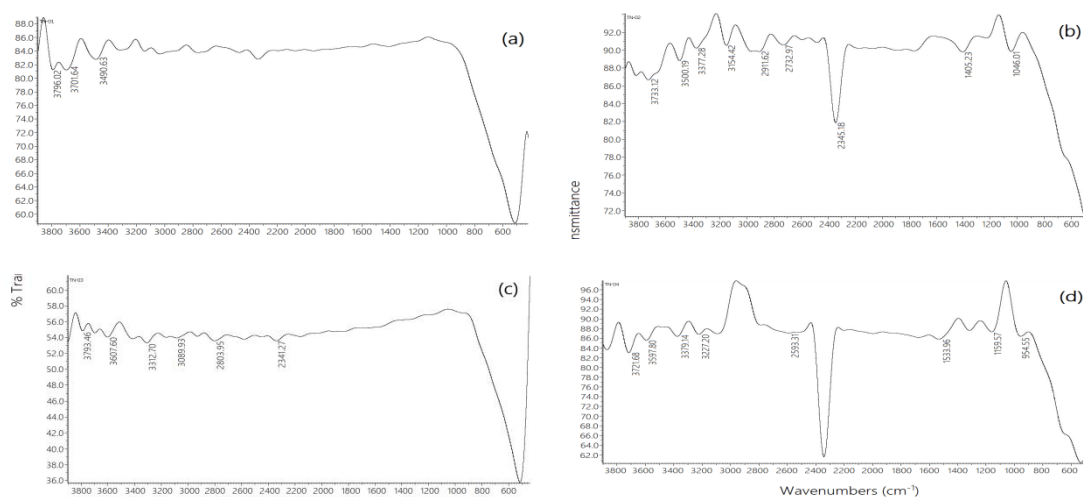


Fig. 3. IR spectra of (a) TN-1; (b) TN-2; (c) TN-3; (d) TN-4

The intensity of spectral features reveal the presence of more surface sites bearing hydroxyl groups and adsorbed water molecules in case of TN-3 and lesser in case of other TN samples. This observation can be related to variation in crystal structure due to difference in calcination temperature. However, TN-2 and TN-4 are found to show a distinct band in the range of 2200-2400 cm^{-1} observed with a slight increment in the intensity in case of TN-4. This sharp

band most likely appears due to the presence of very strong hydrogen bonding between OH groups [16].

These results show that all the TN samples contain surface hydroxyl groups that significantly enhance their catalytic activity by producing reactive OH radicals thereby providing active sites for the adsorption of pollutants [16,35]. Moreover, the identification of Ti–O and Ti–O–Ti bonds among all the samples confirm the formation of titania.

3.4. Field emission scanning electron microscopy

The surface morphology of the prepared samples of titania nanoparticles TN-1 and TN-4 was studied by field emission scanning electron microscopy and images recorded at 100,000x magnification are shown in Figures 4(a & b). The micrographs illustrate surface morphology of small titania particles having spherical shape with a variety of sizes below 100nm combined to form aggregates ranging from a few to several tens of nanometers in size. However, the surface morphology of TN-4 significantly varies from TN-1 since it possesses relatively uniform size and distribution of particles with lesser aggregation.

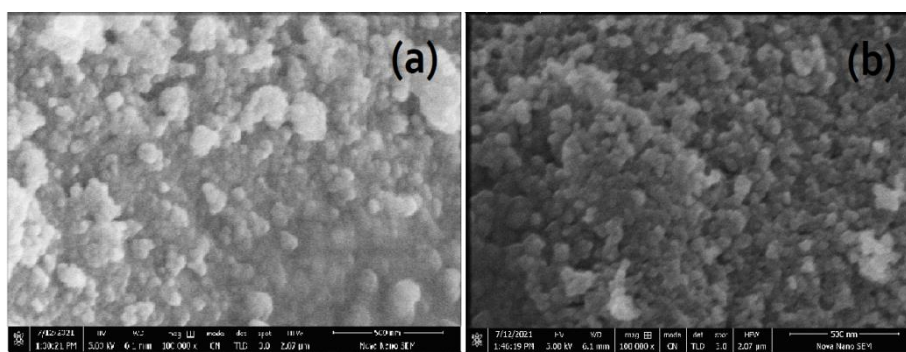


Fig. 4. SEM micrographs of (a) TN-1; (b) TN-4

In fact, the phenomenon of aggregation takes place due to the high surface energy of fine particles that is being lowered during their growth [36]. Also, it is significantly favored by calcination necessary for inducing crystallinity among the nanoparticles [37]. Moreover, titania particles prepared by sol-gel process have been found to be specific in having affinity to agglomerate since the phenomenon of enhanced agglomeration during their formation has been observed quite frequently by the previous scientists [38,39]. According to some researchers the primarily formed small particles interact chemically to form aggregates that further bind with each other through van der Waals forces and hence result in the formation of larger aggregates ranging in micrometer size [40].

3.5. Energy dispersive X-ray spectroscopy

Selected area of TN-1 and TN-4 was subjected to energy dispersive X-ray spectroscopy in order to confirm their elemental composition as weight percentage and spectra are illustrated in Figures 5 (a & b) whereas the percentage composition is reported in Table 1. The table specifies the presence of titanium and oxygen only among both the TN samples. No peak for any other element is observed; this evidence confirms the purity of synthesized titania powders. The weight percentages of titanium and oxygen in case of TN-1 are found to be in close agreement with that of theoretical values i.e. 53.08% and 46.92% respectively. The data shows a significant increase in the percentage of titanium in TN-4 with a successive decrease in the quantity of oxygen probably due to the phase transformation that occurred during the calcination process.

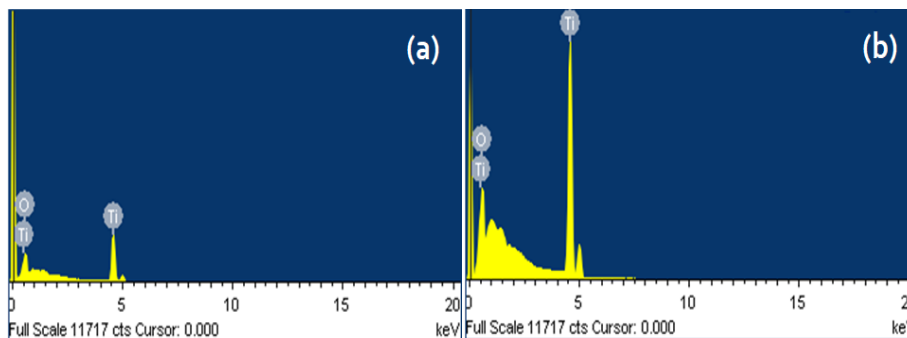


Fig. 5. EDX spectra of (a) TN-1; (b) TN-4.

Table 1. EDX analysis-Elemental compositions of TN samples.

Element	Weight %	
	TN-1	TN-4
O	46.92	38.08
Ti	53.08	61.92

3.6. Wastewater Treatment

Industrial wastewater was treated at 1g/L and 2g/L dosages of TN samples keeping all other parameters constant, i.e. contact time 20 hours, agitation speed 120 rpm and agitation time 4 hours, and results are presented in Tables 2 and 3. The results show slight reduction in COD, BOD and TDS. However, significant reduction in color can be observed with a maximum of 69 to 70% removal in case of TN-1 and TN-2. As the dosage of all the TN samples was increased to 2g/L a slight variation in COD, BOD and TDS reduction can be seen while similar results for the removal of color were obtained.

Tables 4 and 5 show the effect of cyanide concentration and its removal by applying titana samples to cyanide synthetic solution. It can be observed that the increase in concentration from 10 to 20 ppm resulted in enhanced reduction of cyanide i.e. 46.40%, 15.70%, 39.60% and 13.60% for TN-1, TN-2, TN-3 and TN-4 respectively at 1g/L dosage whereas at 2g/L dosage, 55.80%, 19.10%, 32.70% and 17.70% removal was obtained for TN-1, TN-2, TN-3 and TN-4 respectively. Hence, TN-1 showed better results for both titania dosages as well as initial cyanide concentrations. According to the previous researchers cyanide reduction based on adsorption, a surface phenomenon, is dependent on the number of vacant sites present on the surface therefore, the reduction increases with the increase in dosage as in case of TN-1. However, the initial cyanide concentration was not increased further since previous scientists reported that at higher initial cyanide concentration, its removal may be restricted due to the availability of limited number of sites hence, the removal of cyanide decreases with the increase in initial concentration of cyanide [41].

Table 2. Comparison of TN samples and their efficiency against industrial wastewater pollutants at 1 g/L dosage.

Parameters	Before treatment	TN-1		TN-2		TN-3		TN-4	
			% red.		% red.		% red.		% red.
pH	7.53	8.43	--	8.45	--	8.36	--	8.40	--
COD	1260 mg/L	1034	17.94	1058	16.03	1012	19.68	1021	18.97
BOD	783 mg/L	631	19.41	689	12.00	608	22.35	622	20.56
TDS	6737 mg/L	5466	18.86	5522	18.03	5189	22.98	5399	19.86
Color	77.0 PtCo-Hazen	69	10.39	70	9.09	59	23.38	62	19.48

% red. = percentage reduction

Table 3. Comparison of TN samples and their efficiency against industrial wastewater pollutants at 2 g/L dosage.

Parameters	Before treatment	TN-1		TN-2		TN-3		TN-4	
			% red.		% red.		% red.		% red.
pH	7.53	8.44	--	8.47	--	8.34	--	8.39	--
COD	1260 mg/L	1023	18.8%	1040	17.5%	986	21.75	1011	19.76
BOD	783 mg/L	615	21.45	677	13.53	581	25.80	599	23.50
TDS	6737 mg/L	5440	19.25	5505	18.29	5154	23.50	5376	20.20
Color	77.0 PtCo-Hazen	64	16.88	69	10.39	54	29.87	59	23.38

% red. = percentage reduction

Table 4. Comparison of TN samples and their efficiency against cyanide synthetic solution at 1 g/L dosage.

Parameters	Before treatment	TN-1		TN-2		TN-3		TN-4	
			% red.		% red.		% red.		% red.
CN (10 ppm)	10 ppm Abs.0.073	0.049	31.6%	0.0574	21.4%	0.0533	26.9%	0.0698	4.38%
CN (20 ppm)	20 ppm Abs.0.1471	0.078	46.4%	0.1240	15.7%	0.0889	39.6%	0.1276	13.6%

Table 5. Comparison of TN samples and their efficiency against cyanide synthetic solution at 2 g/L dosage.

Parameters	Before treatment	TN-1		TN-2		TN-3		TN-4	
			% red.		% red.		% red.		% red.
CN (10 ppm)	10 ppm Abs.0.073	0.0442	39.4%	0.0514	29.6%	0.0480	34.2%	0.0617	15.5%
CN (20 ppm)	20 ppm Abs.0.1471	0.065	55.8%	0.1190	19.1%	0.0990	32.7%	0.1210	17.7%

4. Conclusions

The titania samples TN-1, TN-2, TN-3 and TN-4 prepared via non-aqueous route of sol-gel technique were found to be of crystalline nature essential for their improved physical properties. X-ray diffraction study revealed that a considerable change in phase at temperature higher than 700°C occurred with almost 50% of anatase titania transformation into rutile phase without the formation of brookite phase as an intermediate. DSC study also confirmed slow transformation to rutile phase at the temperatures above 650 °C with the absence of brookite phase.

IR spectroscopy showed the presence of surface hydroxyl groups that significantly enhance their catalytic activity by producing reactive OH radicals thereby providing active sites for the adsorption of pollutants. SEM analysis revealed agglomerated morphology of the TN samples with slight variation in the size of agglomerates due to the fact that titania nanoparticles prepared by sol-gel process have tendency to agglomerate. EDX analysis confirmed the elemental composition of titania nanoparticles thereby proving their purity.

Hence, 2-ethyl hexanol together with titanium tetrachloride as precursor for titania inhibit the transformation of anatase to rutile phase and increases its stability upto 700°C. The study leads to the conclusion that the process applied was a quite suitable surfactant free approach for the synthesis of high purity titania powders involving the use of a high boiling organic solvent.

The results for wastewater treatment showed minor reduction in COD, BOD and TDS however, significant reduction in color can be observed with a maximum of 69 to 70% removal in case of TN-1 and TN-2 respectively. The results for cyanide reduction indicated TN-1 with maximum removal of 55.80% of cyanide ions at 2g/L dosage.

References

- [1] A. Keiteb, E. Saion, A. Zakaria, N. Soltani, N. Abdullahi, *Appl. Sci.*, 6 (2016).
- [2] A. Karami, *J. Iran. Chem. Soc.*, 7 (2010).
- [3] K. Suttiponparnit, J. Jiang, M. Sahu, S. Suvachittanont, T. Charinpanitkul, P. Biswas, *Nanoscale Res. Lett.* (2010).
- [4] R. Sonawane, S. Hegde, M. Dongare, *Mater. Chem. Phys.* 77 (2003).
- [5] D. Ramimoghadam, S. Bagheri, S. B. Abd Hamid, *Biomed Res. Int.* 2014 (2014).
- [6] N. Shahruz, Milani Moghaddam Hossain, *World Appl. Sci. J.* 12, 1981 (2011).
- [7] A. Ahmad, G. H. Awan, S. Aziz, *Pakistan Eng.* 70, 404 (2006).
- [8] M. Niederberger, *Acc. Chem. Res.*, 40 (2007).
- [9] E. M. Mahdi, M. H. Abdul Shukor, Y. M. S. Meor, P. Wilfred, *J. Nano Res.*, 21 (2012).
- [10] S. K. Kansal, M. Chopra, *Engineering*, 04 (2012).
- [11] S. Ivanov, A. Barylyak, K. Besaha, A. Bund, Y. Bobitski, R. Wojnarowska-Nowak, I. Yaremchuk, M. Kus-Liškiewicz, *Nanoscale Res. Lett.*, 11 (2016).
- [12] H. Yang, K. Zhang, R. Shi, X. Li, X. Dong, Y. Yu, *J. Alloys Compd.*, 413 (2006).
- [13] V. Chaudhary, A. K. Srivastava, J. Kumar, *MRS Proc.*, 1352 (2011).
- [14] P. Escherichia, C. Di Bawah Lampu, P. Menggunakan, N. Tio, Y. Disintesis, M. Kaedah, S. Gel, S. Rahim, S. Radiman, A. Hamzah, *Inactivation of Escherichia coli Under Fluorescent Lamp using TiO₂ Nanoparticles Synthesized Via Sol Gel Method*, 2012.
- [15] M. Hema, A.Y. Arasi, P. Tamilselvi, R. Anbarasan, *Chem. Sci. Trans.*, 2 (2012).
- [16] M. Šćepanović, B. Abramović, A. Golubović, S. Kler, M. Grujić-Brojčin, Z. Dohčević-Mitrović, B. Babić, B. Matović, Z. V. Popović, *J. Sol-Gel Sci. Technol.*, 61 (2012).
- [17] R. Vijayalakshmi, V. Rajendran, *Synthesis and characterization of nano-TiO₂ via different methods*, n.d. www.scholarsresearchlibrary.com.
- [18] S. A. Ibrahim, S. Sreekantan, *Adv. Mater. Res.*, 173 (2010).
- [19] S. Valencia, J. M. Marín, G. Restrepo, *Open Mater. Sci. J.*, 4 (2009).
- [20] A. Styskalik, D. Skoda, C. Barnes, J. Pinkas, *Catalysts* 7 (2017).
- [21] V. Loryuenyong, K. Angamnuaysiri, J. Sukcharoenpong, A. Suwannasri, *ScienceAsia*, 38 (2012).
- [22] M. Niederberger, N. Pinna, *Met. Oxide Nanoparticles Org. Solvents*, 2009.
- [23] M. M. Ba-Abbad, A. H. Amir Kadhum, A. Bakar Mohamad, M. S. Takriff, K. Sopian, D. Ehsan, *Synthesis and Catalytic Activity of TiO₂ Nanoparticles for Photochemical Oxidation of Concentrated Chlorophenols under Direct Solar Radiation*, 2012. www.electrochemsci.org.
- [24] S. Bagheri, K. Shameli, S. B. Abd Hamid, *J. Chem.*, 2013 (2013).
- [25] C.-J. Li, G.-R. Xu, B. Zhang, J. R. Gong, *Appl. Catal. B Environ.*, 115 (2012).
- [26] V. P. M. Shajudheen, K. Viswanathan, K. A. Rani, A. U. Maheswari, S.S. Kumar, *Int. J.*

- Chem. Mol. Eng. **10**, 556 (2016).
- [27] K.Y. Jung, S. Bin Park, J. Photochem. Photobiol. A Chem., 127 (1999).
- [28] Y. Bessekhoud, D. Robert, J. V. Weber, Int. J. Photoenergy, 5 (2003).
- [29] H. Mehranpour, M. Askari, M. S. Ghamsari, H. Farzalibeik, St J. Nanomater., 2010 (2010).
- [30] M.V. Swapna, K. R. Haridas, J. Exp. Nanosci., 11 (2016).
- [31] V. G. Pol, Y. Langzam, A. Zaban, Langmuir, 23 (2007).
- [32] I. Hernández-Perez, A. M. Maubert, L. Rendón, P. Santiago, H. Herrera-Hernández, L. Díaz-Barriga Arceo, V. Garibay Febles, E. Palacios González, L. González-Reyes, L. Cárdenas Norte, C. San Bartolo Atepehuacán, Ultrasonic Synthesis: Structural, Optical and Electrical Correlation of TiO₂ Nanoparticles, 2012. www.electrochemsci.org.
- [33] S. G. Kumar, K. S. R. K. Rao, Nanoscale, 6 (2014).
- [34] Y. Hu, H.-L. Tsai, C.-L. Huang, J. Eur. Ceram. Soc., 23 (2003).
- [35] A. Ocwelwang, L. Tichagwa, A. R. Ocwelwang, Int. J. Adv. Res. Chem. Sci. **1**, 28 (2014).
- [36] N. Srivastava, P. C. Srivastava, Realizing NiO nanocrystals from a simple chemical method, n.d.
- [37] H. R. Saud, S. S. Al-Taweel, J. Chem. Pharm. Res. **8**, 620 (2016).
- [38] H. M. Chenari, C. Seibel, D. Hauschild, F. Reinert, H. Abdollahian, Mater. Res., 19 (2016).
- [39] R. S. Devi, D. R. Venckatesh, D. R. Sivaraj, Int. J. Innov. Res. Sci. Eng. Technol., 03 (2014).
- [40] H. M. Zaid, H. Fakhruddi, F. Y. Yow, N. Razali, Y. K. Dasan, Defect Diffus. Forum, 391 (2019).
- [41] A. H. Jauto, S. A. Memon, A. Channa, A. H. Khoja, EEnergy Sources, Part A Recover. Util. Environ. Eff., 41 (2019).